INTERNATIONAL JOURNAL OF PHARMACEUTICAL, CHEMICAL AND BIOLOGICAL SCIENCES

Available online at www.ijpcbs.com

Research Article

A NEW BIOACTIVE SCHIFF BASE LIGANDS DERIVED FROM AZOSULFAPYRIMIDINE AND THEIR Fe(III), Co(II) AND Ni(II) COMPLEXES: SYNTHESIS, THERMAL, MAGNETIC AND SPECTROSCOPIC CHARACTERIZATION, 3D MODELING AND BIOLOGICAL STUDIES

Tarek MA Ismail*, Abd-elrazak M Tawfik,

Samy M Abu-El-Wafa and Naglaa M Ahmed

Department of chemistry, Faculty of Education, Ain Shams University, Roxy, Cairo, Egypt.

ABSTRACT

New series of Fe (III), Co (II) and Ni (II) complexes of Schiff base ligands HL and H_2L derived from azosulfapyrimidine were synthesized and characterized by elemental, conductance measurements, IR, electronic absorption, EPR spectra and magnetic measurements. 3D modeling of the ligand and its metal complex indicated that the electron density on the azomethine groups are much higher than the azo group therefore coordination would take place via the azomethine group and the azo group does not participate in complex formation. The complexes exhibited different geometrical arrangements. The variation in the geometrical arrangements depends on the nature of both the metal ions and the Schiff base ligands. *The thermo kinetic parameters are calculated* indicates the activated complex is more ordered than the reactants and / or thermal decomposition reaction is slower than normal. The biological activities of the ligands and complexes have been screened in vitro against some bacteria and fungi to study their capacity to inhibit their growth and to study the toxicity of the compounds.

Keywords: New Schiff base complexes, IR, Visible – UV, EPR spectra, Microbiological activity.

INTRODUCTION

Sulfa-drugs are widely used in the treatment of infections, especially for patients intolerant to antibiotics[1]. The coordination chemistry of sulpha drug and their azo derivatives have much attention by virtue of their applicability as potential ligands for large number of metal ions[2]. The metal chelates thus produced have wide applications in the dye industry, as analytical reagents for the micro determination of metals and in biological uses[3]. Sulfonamides were the first drugs found to act selectively and could be used systematically as preventive and therapeutic agents against various diseases[4]. Sulfur ligands are widespread among coordination compounds and are important components of biological transition metal ions complexes[5]. Research on Fe–S complexes has flourished as a result of the discovery that they are present in electron transfer and nitrogen fixing enzymes[5]. Metal complexes with sulfur containing unsaturated ligands are also of a great interest in inorganic and organometallic chemistry, especially due to their potential with novel electrical and magnetic properties[5]. Schiff bases continue to occupy an important position as ligands in metal coordination chemistry[6], even almost a century since their discovery.

Schiff bases have also been shown to exhibit abroad range of biological activities, including antifungal, antibacterial, antimalarial, anti-inflammatory and antiviral properties[7–8]. The study of the reactivity of various types of heteroaromatic containing Schiff bases linked to metal complexes has received a great deal of attention during the past decades[5]. Some transition metal (II) - complexes of biologically active Schiff bases derived from sulfaguani dine, sulphathiazole, sulphisoxazole , sulphadiazine were prepared[6].

Metal ion complexes of Schiff bases derived from o-vaniline with suflanilamide and sulfamerazine were studied[9]. In the present work, new series of Fe(III),Co(II) and Ni(II) complexes of Schiff base ligands HL and H_2L derived from azosulfapyrimidine were synthesized and characterized by elemental, conductance measurements, IR, electronic absorption, EPR spectra and magnetic measurements. The biological activities of the ligands and their complexes were reported.

EXPERIMENTAL

MATERIALS

All chemicals used in the present work were of highest purity available or of analytical reagent grade (AR). The solvents used were either spectroscopic pure from BDH or purified by the recommended method[10].

INSTRUMENTS

The elemental microanalyses of the prepared compounds for their C, H and N contents were performed in the Microanalytical Center, at Cairo University. Infrared spectra were recorded on a Perkin-Elmer FT-IR spectrometer using KBr discs. The UV–Vis spectra were recorded on a SHIMADZU UV - Vis spectrophotometer model V – 550 in the ranged 350 to 600 nm using the Nujol mull technique. The molar conductance of the complexes in DMF solution (10^{-3} M) was measured using Sybron-Barnstead. Conductometer.The magnetic moments of the prepared metal complexes were determined at room temperature by the Gouy method on (TM) Johnson Methey Alpha Products Susceptibility Balance. The thermogravimetric analyses (TGA and DTA) were carried out in a dynamic nitrogen atmosphere (20 ml min^{-1}) with a heating rate of 10 °C min^{-1} using a Shimadzu TGA-50H. Metal contents of EDTA were determined complexometrically using standard EDTA titration. 3D Modeling of the Structures was carried out by the aid of Gaussian 9.0 program.

PREPARATION OF THE SCHIFF BASE COMPOUNDS

Diazotization and coupling

In 1 L beaker, dissolve (82.5 g, 0.33 mol) of sulfapyrimidine (sulfadiazine) in 85 ml of concentrated hydrochloric acid and 85 ml of water. Cool the mixture to 0 °C in an ice–salt bath with stirring and the addition of a little crushed ice. Add during 10–15 min a solution of (24 g, 0.33 mol) of sodium nitrite in 50 ml of water, stir the solution well during the diazotization, and keep the mixture at a temperature of 0–5 °C by the addition of a little crushed ice from time to time. The very soluble diazonium salt is formed. Dissolve(0.33 mol) of acetylacetone or salicylaldehyde in a solution of 21 g of sodium hydroxide in 75 ml water, cool in ice and add the diazotized solution slowly and with stirring. Then add concentrated hydrochloric acid slowly and with constant stirring to the cold mixture until the pH of solution becomes 5.50. Filter the precipitated substances, [4-(1-acetyl-2-oxo-propylazo)-N-prymidin2-yl-benzene-sulfonamide or 4-(3-formyl-4-hydroxy-phenylazo)- N-pyrimidin-2-yl-benzenesulfonamide, with gentle suction, wash with water until free from acid and dried upon filter paper in the air.

Preparation of the Schiff bases HL (L_1 and L_4)

The Schiff bases HL (L_1 and L_4) were prepared by mixing hot solution 60 ^{0}C of 4-(1-acetyl-2-oxo-propylazo)-N-prymidin-2-yl- benzenesulfonamide or 4-(3-formyl-4-hydroxy-phenylazo)-N-pyr- imidin-2-yl-benzene-sulfoneamide (0.33 mol)with hot solution 60 ^{0}C of ethylenediamine(19.8 g, 0.33 mol) in 50 ml ethanol. The mixture was refluxed for 2 h. The formed solid product was separated by filtration, purified by crystallization from ethanol, washed several times with diethyl ether and dried in vacuum over anhydrous calcium chloride to give orange crystals, yield 80%.

Preparation of the Schiff bases H_2L (L_2, L_3, L_5 and L_6)

Salicylaldehyde or acetylacetone (0.33 mol) was added drop wise to HL_1 or HL_4 (0.33 mol) in absolute ethanol (50 ml). The reaction mixture was refluxed on a hot plate for 4 h. The product was allowed to cool till room temperature, filtered off and recrystallized from ethanol then dried under vacuum to give yellow crystals, yield 85%.

The ligands under investigations were characterized by the elemental and thermal analyses, IR, UV/Vis., Mass ^{1}HNMR spectroscopy and the detailed structure investigation was discussed elsewhere[11]. The ligands have the following structural formulae:

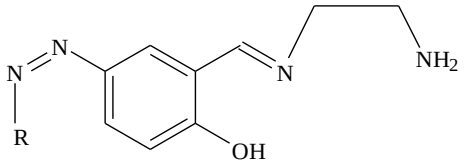

4-{3-[(2-Amino-ethylimino)-methyl]-4-hydroxy-phenylazo}-N-pyrimidin-2-yl-benzenesulfonamide [AEMHPPS]. **L_1**

Where R =

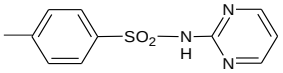

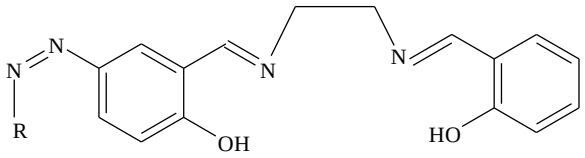

4-(-Hydroxy-3-{[2-(1-methyl-3-oxo-butylideneamino)-ethylimino]-methyl}-phenylazo)- N-pyrimidin-2-yl-benzenesulfonamide [HMOEMPS]. **L_2**

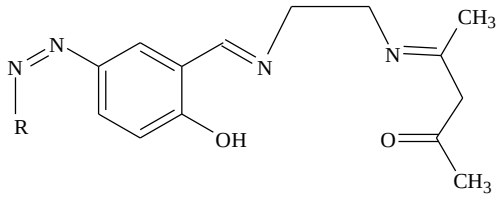

4-[4-Hydroxy-3-({2-[(2-hydroxy-benzylidene)-amino]-ethylimino}-methyl)-phenylazo]- N-pyrimidin-2-yl-benzenesulfonamide [HHEMPS]. **L_3**

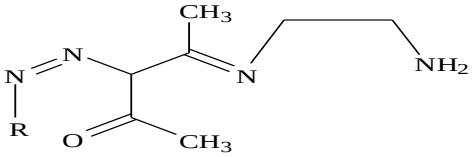

4-[1-Acetyl-2-(2-amino-ethylimino)-propylazo]-N-pyrimidin-2-yl-benzebesulfonamide [AAPPS]. **L_4**

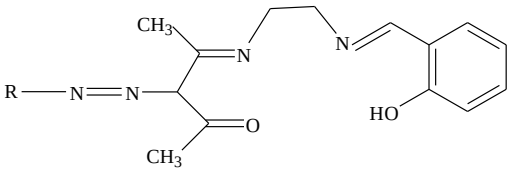

4-(1-Acetyl-2-{2-[(2-hydroxy-benzlidene)-amino]-ethylimino}-propylazo)-N-pyrimidin-2-yl-Benzenesulfonamide [AHAPPS]. **L_5**

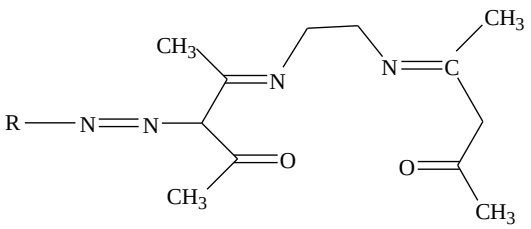

4-{1-Acetyl-2-[2-(1-methyl-3-oxo-butylideneamino)-ethylimino]-propylazo}- N-pyrimidin-2-yl-benzenesulfonamide [AMOPPS].**L_6**

SYNTHESIS OF THE METAL ION COMPLEXES

Metal ion complexes of HL and H_2L ligands were prepared by the addition of a hot solution 60 °C of the appropriate metal chloride, sulfate or nitrate (1 or 2 mmol) in ethanol (25 ml) to the well stirred hot solution of the Schiff bases (1 or 2 mmol) in the same solvent (25 ml).The mixture was left under reflux with continuous stirring for 5 hrs where upon the solid complexes precipitated. The obtained solid complex was washed with ethanol followed by diethyl ether and dried in vacuum over anhydrous calcium chloride. The analytical data of the complexes are collected in Table 1

BIOLOGICAL STUDY

Bacteria media

Nutrient agar medium was prepared by standard methods[12-14]. The antibacterial activity of the ligand and its complexes were tested using paper disc diffusion method[15] against gram positive bacteria (Staphylococcus aureus); gram negative bacteria (Escherichia coli), the tested compound in measured quantities were dissolved in DMF to get concentration of 1000 ppm of compounds. Nutrient Agar media was poured in each Petri dish. After solidification, 0.1 ml of the tested bacteria spread over medium using a spreader. The discs of whatman no.1 filter paper having diameter of 5.00 mm., containing compounds were placed in the inoculated Petri plates. The plates are incubated at 28 ^{0}C for 24 - 48 hrs. and the zone of inhibit-ion was calculated in millimeters carefully.

Fungus media

The tested compound in measured quantities was dissolved in DMF to get concentration of 1000 ppm of compounds. Czapek dox agar medium was prepared by standard method[12-16]. Candida albicans and Aspergillus flavus was spread over each dish by using a sterile bent loop rod. Disks were cut by sterilized cork borer and then taken by sterilized needle. The resulting pits are sites for the test compounds, the plates are sites for the tested compounds. The plate is incubated at 30^{0}C for 24 – 48 hrs and the any clear zones present were detected, the zone of inhibition was calculated in millimeters carefully.

RESULTS AND DISCUSSION

Characterization of the ligands

The structures of the prepared Schiff bases were investigated by the IR, ^{1}H NMR and UV/Vis spectra. The IR spectra of the Ligands show characteristic bands at 3522–3530 cm^{-1} (L_1, L_2, L_3 and L_5) and 2975–2980 cm^{-1} (L_3, L_4, L_5 and L_6) corresponding to γ_{OH} phenolic and γ_{OH} enolic, respectively[17]. The ligands L_1 and L_4 show bands at 3310–3330 and 3280–3290 cm^{-1}due to γNH_2 asy and γNH_2 sym. The bands at 1640–1649 and 1625-1630 cm^{-1} for all ligands can be assigned to γ C=N free and γ C=N bonded (in H-bonding with OH group) [17]. All ligands show bands at 1535–1540, 1435–1450, 1321–1328 and 1155–1158 cm^{-1} due to γ C=N ring, γ N=N, γ SO_2 asy and γ SO_2 sym, respectively. ^{1}H NMR spectral data of the ligands relative to TMS in DMSO-d_6 without and with D_2O give further support of the suggested structures of the ligands. The aromatic proton signals appeared at 6.02–8.99 ppm, the proton signals of OHphenolic and OHenolic groups at 11.27–11.54 ppm completely disappeared on adding D_2O. The methylene proton signals appeared at 2.51–2.53 and 3.36–3.72 ppm. The UV–vis spectra of the ligands show three bands in the range 220–235, 281–296 and 375–390 nm which can be assigned to π–π* transitions within the aromatic rings, π–π*transitions within C=N and intramolecular charge transfer (CT) transition with the whole molecule.

Characterization of the metal complexes

The complexes under investigations are soluble in DMF and DMSO, partially soluble in methyl and ethyl alcohol and the complexes are insoluble in chloroform, acetone, diethyl ether, benzene, petroleum ether and isopropyl alcohol.

Elemental Analysis

Table 1 , shows, the results of the elemental analysis of the complexes under investigation , the color ,the chemical formula, the percentage of elemental analysis[% calculated (% found)] and the conductance measurements are calculated and listed in the same Table.

3D Modeling Structures

3D modeling of the ligand L_1 using Gaussian 9.0 program Fig.1 indicateds that the electron density on the azomethine groups are much higher than the azo group therefore coordination would take place via the azomethine group and the azo group does not participate in complex formation.

Also, Fig. 2 show 3D modeling of the ligand L_1 and its Co(II) complex (1) using Gaussian 9.0 program , on comparing the electron density function of ligand (a) and Co(II) complex (b) the following can pointed out:

i) The electron density function of azo group either on ligand or Co(II) complex is the same, this indicate the azo group does not play any role in formation of Co(II) complex.

ii) The electron density function of azomethine group in ligand (a) is higher than of the azomethine density function of the Co(II) complex (b), this indicates the azomethine group participate in formation of Co(II) complex. This conclusion is confirmed from IR spectra of ligand L_1 and its Co (II) complex where the C=N of the ligand is shifted to lower frequency in the IR spectra of Co(II) complex. The shift in IR spectra to lower values indicates the participation of C=N groups in formation of Co(II) complex.

IR – spectra

On comparing the IR – spectra of the free ligands with those of their metal ion complexes the following can be pointed out:

I) The $\gamma_{C=N}$ bonded of the free ligands are absent in the spectra of the complexes , whereas, the $\gamma_{C=N}$ of the free ligands , is shifted to lower wave number by 15 – 21 cm^{-1} in the IR spectra of the complexes. This means that the C = N group is involved in coordination to Co(II), Ni(II) and Fe(III) in their complexes. These conclusions are in line with the data obtained from electrostatic potential studies that the azomethine groups have higher in electron density than the azo group.

ii) In the IR spectrum of the free ligands the γ_{OH} phenolic (L_1, L_3 ,L_5 and L_6) and γ_{OH} enolic (L_2, L_3, L_4 and L_6) are absent from the IR spectra of the complexes which indicates that ,the phenolic (OH) and enolic (OH) groups contribute to the formation of complexes by H^+ ions displacement[17], which points out that the free ligands contribute to complex formation as monoanionic or dianionic ligands

iii) In the IR spectra of all complexes the strong to medium broad bands appearing in the ranges 800-840cm^{-1}, which are not present in the IR spectra of the free ligands, can be assigned to γ_{H2O} associated with the complex formation.

iv) The out of plane deformation bands of water molecules appearing near 840 cm^{-1} are due to $\rho(H_2O)$, whereas the $\omega(H_2O)$ appears near 800 cm^{-1}.

v) The IR spectra indicate that the bands of $\gamma_{NH2\ asym}$, $\gamma_{NH2\ sym}$ γ (NH asym), γ (NH sym), $\gamma_{C=N}$ ring (asym), $\gamma_{C=N}$ ring (sym), $\gamma_{N=N\ asym}$, $\gamma_{N=N\ sym}$, γ_1 SO_2, γ_2 SO_2 and γ_3 SO_2 respectively in the IR spectrum of the free ligands still lie at the same position in the IR spectra of the complexes. This indicates that these groups did not contribute to the coordination to the metal ions in the complexes.

vi) For all complexes two new bands appear in their IR spectra at 444 – 478 cm^{-1} and 344 – 383 cm^{-1} respectively which are absent from the IR spectra of the free ligands , these can be assigned to γ_{M-O} and γ_{M-N} bands respectively[18].

vii) In the IR – spectra of the complexes (2) and (9) two new bands appear at 1050 – 1056 and 1280 - 1285 cm^{-1} respectively, which correspond to γ_{OH} and ∂ OH of the OH group associated with complex formation. These bands are absent from the IR – spectra of the free ligands and also from the IR – spectra of the other complexes. The existence of these bands is a proof for the presence of the $(OH)^-$ group bonded to the nickel or ferric ion to compensate the positive charge that remains on the ferric ion after the reaction with the ligand. This finds further support by the absence of the other anions in the complex.

Molar conductance

The molar conductance of the metal ion complexes under investigation are measured for 10^{-3} M solution in DMF. The results of molar conductance are listed in Table (1) and indicate that all the complexes under investigation are non- electrolytes [19].

The Electronic Absorption Spectra of the Complexes

The electronic absorption spectra of the metal complexes under investigation were recorded within the range 350-800nm applying the Nujol mull technique and DMF solution. The data of the Ni(II), Co(II)and Fe(III)complexes obtained from these spectra are recorded in Table (2). All the solid complexes (1 - 14) under investigation are readily soluble in DMF, so it is easy to prepare solutions from the solid complexes and measure their absorption spectra, whereas the Nujel mull technique is applied in order to obtain the visible absorption spectra for the various complexes as solid suspension.

It is well known that Ni(II) ions form a large number of complexes whose coordination number varies from four to six[20-21]. The structure of the six coordinate complexes are generally octahedral with slight distortion while those with coordination number four mostly have square planar arrangement[22], though tetrahedral geometry has been reported for some complexes[20]. For the [Ni (AEMHPPS) (OH) $(H_2O)_2$].$3H_2O$, complex (2) and [Ni (AAPPS)$_2$ $(H_2O)_2$] complex (8) , the spectra show no difference

between Nujol mull and DMF . These bands are assigned to $^3A_{2g} \rightarrow {}^3T_{1g}$ (F), $^3A_{2g} \rightarrow {}^3T_{1g}$ (P) transition in an octahedral structure of the complexes . Nickel (II) complexes (2) and (8) show tow bands at 535 – 550 and 740 – 770nm ranges, which attributable to $3A_{2g}$ (F) $\rightarrow {}^3T_{1g}$ (F) (ν_1) and $^3A_{2g}$ (F) $\rightarrow {}^3T_{2g}$ (F) (ν_2) transitions respectively, indicating octahedral structure. The ν_2 / ν_1 ratio for the complexes (2) and (8) are 1.38 and 1.40, which are less than the usual range of 1.50 – 1.75, indicating distorted octahedral nickel (II) complexes[22]. In case of [Ni (AMOPPS)].½H_2O , complex (13), the spectra show one band in Nujol mull and DMF at 620 and 650 nm respectively, which can be assigned to $^3T_1 \rightarrow {}^3T_1$(P) transition corresponding to tetrahedral structure in the solid state and changed into octahedral structure in DMF solution[23].

The electronic absorption spectra of the Co (II) complexes namely, [Co (AEMHPPS)$_2$(H_2O)$_2$]. H_2O, complex (1), [Co (HHEMPS)$_2$(H_2O)$_2$]. H_2O, complex (4), [Co (HMOEMPS). (H_2O)$_2$], complex (6) and [Co (AHAPPS)(H_2O)$_2$] complex (10), show bands at 625, 640 , 650 and 635nm in DMF solution and in Nujol mull at 620, 630 and 640and630 nm respectively corresponding to $^4T_{1g}$ (F) $\rightarrow {}^4A_{2g}$(P) and $^4T_{1g}$(F) $\rightarrow {}^4T_{1g}$(P) transitions indicating octahedral structure[24]. whereas the electronic absorption spectra in case of [Co(AAPPS)$_2$], complex (7) and [Co[(AMOPPS)].(½H_2O) , complex (12) shows no obvious changes in the bands of the spectra in Nujol mull or in DMF solution at 690 or 685 respectively assigned to $^4A_2 \rightarrow {}^4T_1$ (P) transition indicating tetrahedral structure around central Co(II) ion[24].

The absorption spectra of all Fe(III) complexes namely, Fe[(AEMHPPS)$_2$(OH)(H_2O)] , complex (3), [Fe (HHEMPS)$_2$ (OH) (H_2O)] , complex (5), [Fe (AAPPS)$_2$(OH) (H_2O)] , complex (9), [Fe (AHAPPS).(OH) (H_2O)],complex (11) and [Fe (AMOPPS) (OH) (H_2O)], complex (14) show bands in Nujol mull at 610 - 635nm but the bands in DMF solution are located at 620-670nm .These bands correspond to $^6A_{1g} \rightarrow {}^4T_{2g}$ (D) transitions for a octahedral structure[15].

Magnetic moment

The effective magnetic moments of the prepared metal complexes were determined; the data obtained are listed in Table 2**.** The observed magnetic moment of the Fe(III) complexes 3,5 9,11 and 14 were found to be 5.31, 5.90 ,5.33 , 6.00 and 5.64 B.M. respectively (theoretical spin only value 5.91 B.M.) which means five unpaired electrons are present in the d – orbital with high spin octahedral geometry [25] through sp^3d^2 hybridization of Fe(III) ion.

The values of the observed magnetic moment of the Co(II) complexes 1,4,6,7 ,10 and 12 amount to 3.77, 3.77, 3.36, 3.41, 3.29 and 3.06 B.M. respectively . These values show the presence of three unpaired electrons in the d – orbital. Therefore the Co(II) complexes have either the tetrahedral geometry with sp^2d hybridized d – orbital in complexes 7 and 12 or an octahedral geometry through sp^3d^2 hybridized d – orbital as in the complexes1, 4, 6, and 10. These values of $\mu_{eff.}$ reveal some weak spin – spin coupling in these complexes[26].

All the investigated Ni(II) complexes 2, 8, and 13 show paramagnetic behavior with magnetic moment 2.80, 2.74, and 2.67 B.M. respectively. These values show the presence of two unpaired electrons in the d – orbital**,** therefore, the complexes formed have either tetrahedral geometry with sp^2d hybridized d – orbital as in complex (13) or an octahedral geometry through sp^3d^2 hybridized d – orbital as in complexes (2) and (8)[27].

Thermogravimetric analysis (TGA, DTA, and DTG) studies

The TGA, DTA and DTG curves of the prepared metal complexes were recorded from ambient temperature up to 800 ^{0}C under N_2 gas flow at heating rate of 30 ^{0}C/min. The thermograms of some Co(II) complexes are shown in Fig.3. The results are summarized in Table 3.

It is clear from TGA, DTA and DTG curves of complex 1 ,complex 6 and complex 12 Fig.3, and the data in Table 3 that each endothermic or exothermic peak on the DTA curve are corresponding to certain chemical transformation . This is accompanied by an inflection on the TGA curve or a strong peak on DTG curve from which corresponding weight loss or heat transformation can be calculated. The curves show mass loss in weight corresponds to the volatilization of one lattice and two coordinated water molecules for complex 1, two coordinated water molecules for complex 6 and half lattice water molecule for complex 12

The TGA, DTG and DTA curves of the complexes 1, 6, and 12 show thermal stability up to temperature 190 – 350, , 210- 405 and 350 - 650 ^{0}C respectively . This means that the complex12 is the most thermally stable complex whereas the complex 1 is the least thermally stable complex in the series. The thermal stability of the Co (II) complexes can be arranged according to their thermal stabilities in the following order:

Complex 12 > 6 >1

The complexes under investigation undergo decomposition of the organic ligand within the temperature ranges 270 – 315 ^{0}C, 315 – 600^{0}C and 600 – 800 ^{0}C for complex 1, , 295 – 460 ^{0}C and 460 – 800 ^{0}C for complex 6 , 310 – 350 ^{0}C, 350 – 500 ^{0}C and 500 – 800 ^{0}C for complex 12. Further mass loss are observed for all the complexes under investigation at temperature > 800 ^{0}C leading to formation of Co (II) oxalate complexes.

The DTA curves of Co (II) complexes show the removal of lattice water as represented by the small endothermic peaks within the temperature range 21 – 96.6 ^{0}C. The exothermic or endothermic peaks within the range 120 – 130.76 ^{0}C are due to elimination of the coordinated water molecules in case of complex 1 and complex 6. The exothermic peaks within the temperature range 193 – 320 ^{0}C are due to some lattice rearrangements taking place at the beginning of the melting of the anhydrous complex or the phase transformation leading to the formation of the corresponding Co (II) oxalate complexes as final products at temperature > 800 ^{0}C.

The order (n), the activation energy (ΔE_a) and the kinetic parameters (ΔH^0, ΔS^0 and ΔG^0) of the thermal decomposition steps for the complexes under investigation were determined from TGA results using the coats – Redfern relations[28]. From the data in Table 2, the following remarks can be pointed out:

1. The ΔS^0 values were found to be negative. The negative sign of ΔS^0, as are discussed previously by some authors,[29-30] indicates the contribution of some other processes with negative entropy which exceeds that of the water removal reaction. This indicates the activated complex is more ordered than the reactants and / or thermal decomposition reaction is slower than normal[31]. This is in good agreement with that reported earlier for some divalent Co(II) Schiff base complexes[32-33]. The thermal decomposition of Schiff base complexes showed the presence of two or three distinct stages for the TG – curves. The first stage was explained by the evolution of the lattice or coordinated water molecules which was followed by decomposition of the anhydrous complexes to give Co (II) oxalate as intermediate fragment in the second stage.
   There are no obvious trends in the heat of the activation of enthalpies ΔH^0. However, the activation energy ΔG^0 increases for the subsequent decomposition stages of a given complex. This may be due to the incorporation of $T\Delta S^0$ term in ΔG^0 which increase significantly from one step to another. This reflects the incorporation of the entropy term at high temperature in the thermal decomposition of the complexes
2. There are no obvious trends in the heat of the activation of enthalpies ΔH^0. However, the activation energy ΔG^0 increases for the subsequent decomposition stages of a given complex. This may be due to the incorporation of $T\Delta S^0$ term in ΔG^0 which increase significantly from one step to another. This reflects the incorporation of the entropy term at high temperature in the thermal decomposition of the complexes.
3. The thermal decomposition stages of all complexes under study obey, in the most cases, first order kinetics.

EPR Spectra

The EPR spectra of complexes (1), (9), (11) and (14) are recorded at room temperature in the solid state and are seen in Fig.4. The geff values calculated of some Co (II) and Fe (III) complexes are listed in Table 1. The EPR spectra of complex (1) show a broad signal. The shape of the EPR signal and the pattern of the $g_{eff.}$ value may indicate octahedral geometry around Co (II) ion.

According to Fidone and Stevense[34] the negative contribution from the free electron 2.0023 ,may be due to increase in the percentage of the ionic character in the covalent bond between ligand and Co(II)ion.

The EPR spectra of complex (9) , complex (11) and complex (14) display a broad signal , the shape of the signals and the pattern of the $g_{eff.}$ obvious hyperfine structure are characteristic of high spin d^5 Fe(III) in octahedral environment . Also those indicate that the Fe(III) ion is existing in different bonding environments . The negative deviation in the $g_{eff.}$ value of the complex under investigation than the value of the free electron, 2.0023, may account for partial ionic character in the bonding of the Fe (III) ion to ligand[35-36].

Based on the above knowledge gained from elemental, IR, electronic, and EPR spectra together with the data of magnetic moments, the bonding between Co (II), Ni (II) and Fe (III) ions and the ligands under investigation may have the following structures:

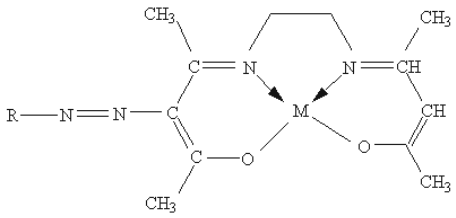

Complex (!2) , M = Co
Complex (13) , M = Ni

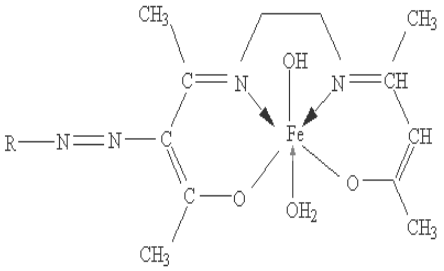

Complex (14)

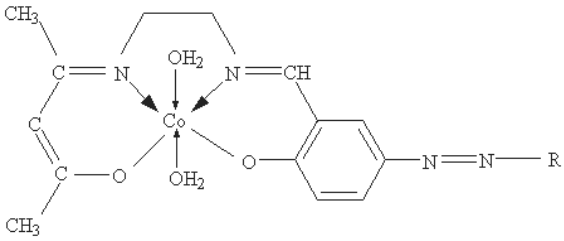

Complex (6)

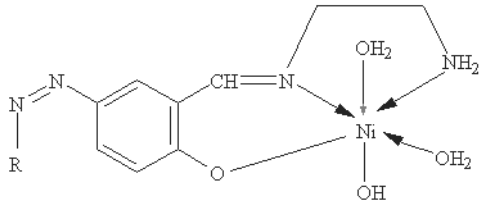

Complex (2)

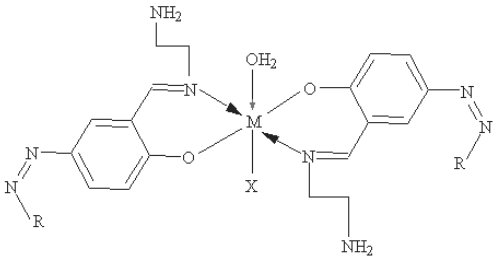

Complex (1), M = Co, X = H 2O
Complex (3), M = Fe , X = OH

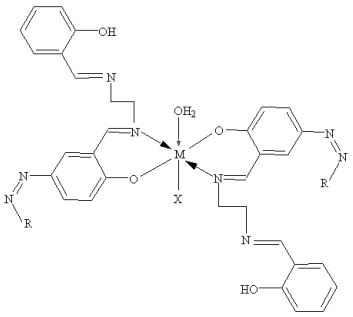

Complex (4), M = Co, X = H 2O
Complex (5), M = Fe , X = OH

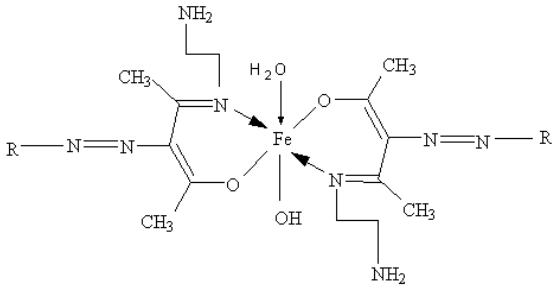

Complex (9)

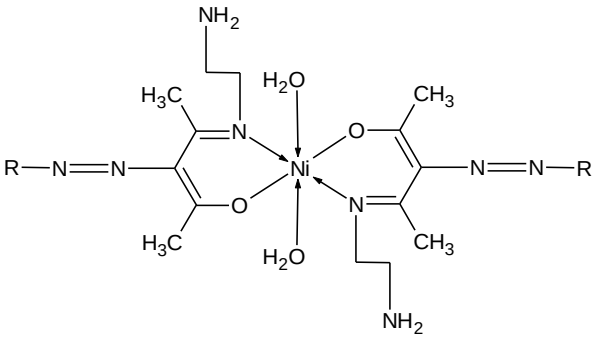

Complex (8)

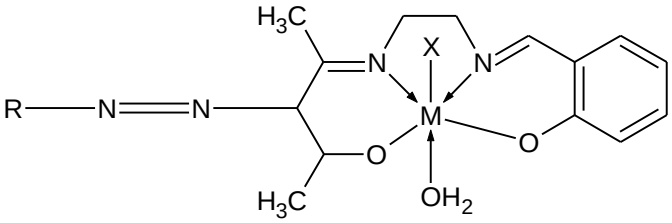

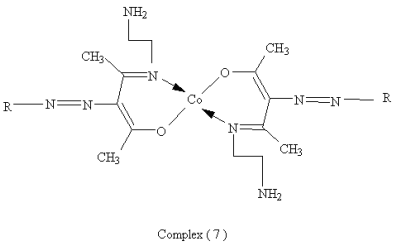

Complex (7)

Complex (10), M=Co, x=H_2O
Complex (11), M=Fe, X=OH

BIOLOGICAL STUDIES

Antibacterial and antifungal activity of the ligands (L_1 – L_4) and their complexes were tested, the results are collected in Table 4 and Fig.5.The results show the metal chelates exhibit more inhibitory effects than the parent ligand. From the data obtained it is observed that, the inhibition zone area is much larger for metal complexes against the gram positive bacteria (Staphylococcus aureus); gram negative bacteria (Escherichia coli) and fungi (Aspergillus flavus and Candida albicans). The increased activity of the metal chelates can be explained on the basis of chelation[37] potent bactericidal agents and to antifungal agent, thus killing more of the bacteria than the ligand. It is observed that, in a complex, the positive charge of the metal is partially shared with the donor atoms present in the ligand, and there may be π-electron delocalization over the whole chelating[38]. This increases the lipophilic character of the metal chelate and favours its permeation through the lipoid layer of the bacterial membranes. Also, there are other factors which also increase the activity, such as solubility, conductivity and bond length between the metal and the ligand. The mode of action may involve the formation of a hydrogen bond through the azomethine nitrogen and oxygen atom with the active centers of the cell constituents, resulting in interference with the normal cell process. The variation in the effectiveness of different compounds against different organisms depend either on the impermeability of the cells of the microbes or the difference in ribosoms of microbial cells[39]. There is a marked increase in the activities of the ligands and complexes for gram positive bacteria (Staphylococcus aureus) gram-negative bacteria (Escherichia coli) and fungi (Aspergillus flavus and Candida albicans).

The order of activities of Staphylococcus aureus are:

Complex5 > complex3 = complex 9 > L_4 > L_2 > L_3 = L_1 > complex 1 > complex 4 = complex 8 > complex 10

The orders of activities of Escherichia are:

Complex3 > = complex 5 > L_4 = complex 9 = L_2 > L_3 > L_1 = complex 4 > complex1 = complex 8 > complex 10.

The order of activities of Candida albicans are:

Complex3 = complex 9 > complex 5 > L_4 =complex 4 > L_1 > complex1 = L_3 = L_2 > complex 8 = complex 10.

The order of activities of Aspergillus flavus are:

Complex 9 = complex5 > complex 3 > L_1 = complex1 = L_4 > complex 4 > L_2 = L_3 = complex 10 > complex 8.

Upon comparison of the biological activity under investigation of the Schiff bases and their metal complexes with the biological activity of lanthanides Schiff base complexes derived from sulfa derivatives[40] and the activity of other Schiff base complexes situated in literature as indicated elsewhere[41-42] the following can be pointed out:

i) The microbiological activity of the Schiff base complexes under investigations show higher biological activity towards gram positive bacteria (Staphylococcus aureus) gram-negative bacteria (Escherichia coli) and fungi (Aspergillus flavus and Candida albicans) as indicated for other Schiff base ligands and their metal complexes[43- 44]

ii) The importance of this unique property of the investigated Schiff base complexes is that they could be administered safely for the treatment of infections caused by any of these particular strains.

ii) Therefore, it is claimed here that such compounds might have a possible antitumor effect since Gram-negative bacteria are considered a quantitative microbiological method for testing beneficial and important drugs, in both clinical and experimental tumor chemotherapy[43-44].

CONCLUSION

Bioactive Schiff base ligands and their Co (II), Ni (II) and Fe (III) complexes derived from azosulfapyrimidine were prepared and characterized by different spectroscopic techniques, molar conductance and magnetic measurements. There are varieties in the geometrical structures of the prepared metal complexes: tetrahedral and octahedral structures. The thermal decomposition as well as the thermodynamic parameters is studied. Antibacterial and antifungal activity of the ligands and their complexes were tested. The metal chelates exhibit more inhibitory effects than the parent ligand.

Table 1: Analytical and Physical Data of Fe (III), Ni (II) and Co(II) Complexes

NO.	Complexes	Molecular Formula	Color	Elemental Analysis % Calculated (% Found)				Ω Ohm^{-1} Cm^2 mol^{-1}
				% C	% H	% N	% M	
1	[Co (AEMHPPS)$_2$(H$_2$O)$_2$]. H$_2$O	Co($C_{19}H_{18}N_7O_3S$)$_2$. 3H$_2$O	Pale reddish Brown	47.45 (47.58)	4.37 (4.17)	20.4 (20.95)	6.13 (5.9)	13.35
2	[Ni (AEMHPPS) (OH) (H$_2$O)$_2$].3H$_2$O	Ni($C_{19}H_{18}N_7O_3S$).OH.5H$_2$O	Orange	38.64 (38.00)	4.91 (5.27)	16.61 (17.00)	10.00 (10.33)	20.00
3	[Fe (AEMHPPS) $_2$.(OH).(H$_2$O)]	Fe ($C_{19}H_{18}N_7O_3S$)$_2$.OH H$_2$O	Brown	48.56 (48.53)	4.15 (4.27)	20.87 (21.10)	5.96 (5.6)	19.00
4	[Co (HHEMPS)$_2$(H$_2$O)$_2$]. H$_2$O	Co($C_{26}H_{21}N_7O_4S$)$_2$.3H$_2$O	Reddish Brown	53.74 (53.7)	4.13 (3.81)	16.90 (16.01)	5,08 (5.90)	15.59
5	[Fe (HHEMPS)$_2$.(OH).(H$_2$O)]	Fe ($C_{26}H_{21}N_7O_4S$)$_2$OH.H$_2$O	Brown	55.50 (55.91)	3.93 (3.74)	17.12 (17.72)	4.89 (4.90)	19.6
6	[Co(HMOEMPS). (H$_2$O)$_2$]	Co ($C_{24}H_{23}N_7O_4S$).2 (H$_2$O)	Reddish Brown	48.0 (4.83)	4.5 (4.6)	16.33 (17.00)	9.83 (10.32)	10.36
7	[Co(AAPPS) $_2$]	Co ($C_{17}H_{20}N_7O_3S$)$_2$	Paige	47.27 (47.27)	4,63 (4.22)	22.71 (22.00)	6.83 (6.79)	16.64
8	[Ni (AAPPS) $_2$ (H$_2$O)$_2$]	Ni[($C_{17}H_{20}N_7O_3S$)$_2$. 2(H$_2$O)	Yellow	45.43 (45.04)	4. 99 (4.84)	19.82 (20.24)	6.46 (6.20)	12.82
9	[Fe (AAPPS)$_2$(OH). (H$_2$O)]	Fe ($C_{17}H_{20}N_7O_3S$)$_2$ OH.H$_2$O	Yellow	45.59 (46.08)	4.80 (4.52)	21.90 (21.76)	6.26 (6.30)	14.04
10	[Co (AHAPPS).(H$_2$O)$_2$]	Co ($C_{24}H_{23}N_7O_4S$).2(H$_2$O)	Yellow	48.00 (48.00)	4.53 (4.45)	16.33 (16.12)	9.83 (9.58)	13.4
11	[Fe (AHAPPS).(OH). (H$_2$O)]	Fe($C_{24}H_{23}N_7O_4S$).(OH).H$_2$O	Yellow	48.32 (48.48)	4.36 (4.55)	16.44 (16.50)	9.39 (9.38)	15.56
12	[Co (AMOPPS)].(½H$_2$O)	Co ($C_{22}H_{25}N_7O_4S$).½ (H$_2$O)	Yellow	47.91 (48.16)	4.72 (4.98)	17.78 (16.92)	10.70 (10.32)	14.4
13	[Ni (AMOPPS)].(½H$_2$O)	Ni ($C_{22}H_{25}N_7O_4S$). (½H$_2$O)	Paige	47.91 (48.11)	4.72 (5.01)	17.79 (18.06)	10.70 (10.90)	16.56
14	[Fe (AMOPPS).(OH).(H$_2$O)]	Fe ($C_{22}H_{25}N_7O_4S$).(OH) H$_2$O	Yellow	46.00 (46.18)	4.87 (4.68)	17.07 (17.12)	9.76 (9.80)	19.45

Table 2: UV- visible spectra, g_{eff} and Magnetic Moment data of the complexes

No.	complexes	$\lambda_{max.}$(nm)		d-d assignment	$\mu_{eff.}$ B.M.	g_{eff}
		In DMF solution	In Nujol mull			
1	[Co (AEMHPPS)$_2$(H$_2$O)$_2$]. H$_2$O	625	620	$^4T_{1g}(F) \rightarrow {}^4A_{2g}(P)$, $^4T_{1g}(F) \rightarrow {}^4T_{1g}(P)$	3.77	1.85
2	[Ni (AEMHPPS) (OH) (H$_2$O)$_2$].3H$_2$O	535 , 740	535 , 740	$^3A_{2g} \rightarrow {}^3T_{1g}(F)$, $^3A_{2g} \rightarrow {}^3T_{1g}(P)$	2.8	
3	[Fe (AEMHPPS) $_2$.(OH).(H$_2$O)]	620	610	$^6A_{1g} \rightarrow {}^4T_{2g}(D)$	5.3	
4	[Co (HHEMPS)$_2$(H$_2$O)$_2$]. H$_2$O	640	630	$^4T_{1g}(F) \rightarrow {}^4A_{2g}(P)$,$^4T_{1g}(F) \rightarrow {}^4T_{1g}(P)$	3.77	
5	[Fe (HHEMPS)$_2$.(OH).(H$_2$O)]	670	635	$^6A_{1g} \rightarrow {}^4T_{2g}(D)$	5.9	
6	[Co(HMOEMPS). (H$_2$O)$_2$]	650	640	$^4T_{1g}(F) \rightarrow {}^4A_{2g}(P)$, $^4T_{1g}(F) \rightarrow {}^4T_{1g}(P)$	3.36	
7	[Co(AAPPS) $_2$]	690	690	$^4A_2 \rightarrow {}^4T_1(P)$	3.41	
8	[Ni (AAPPS) $_2$ (H$_2$O)$_2$]	550 , 770	550 , 770	$^3A_{2g} \rightarrow {}^3T_{1g}(F)$, $^3A_{2g} \rightarrow {}^3T_{1g}(P)$	2.74	
9	[Fe (AAPPS)$_2$(OH). (H$_2$O)]	665	635	$^6A_{1g} \rightarrow {}^4T_{2g}(D)$	5.32	1.93
10	[Co (AHAPPS).(H$_2$O)$_2$]	635	630	$^4T_{1g}(F) \rightarrow {}^4A_{2g}(P)$ and $^4T_{1g}(F) \rightarrow {}^4T_{1g}(P)$	3.29	
11	[Fe (AHAPPS).(OH). (H$_2$O)]	660	630	$^6A_{1g} \rightarrow {}^4T_{2g}(D)$	6.00	1.96
12	[Co[(AMOPPS)].(½H$_2$O)	685	685	$^4A_2 \rightarrow {}^4T_1(P)$	3.06	
13	[Ni (AMOPPS)].(½H$_2$O)	650	620	$^3T_1 \rightarrow {}^3T_1(P)$	2.67	
14	[Fe[(AMOPPS).(OH).(H$_2$O)]	640	625	$^6A_{1g} \rightarrow {}^4T_{2g}(D)$	5.64	1.98

Table 3: Results of Thermal Decomposition and Thermal Parameters for Co(II) and Ni(II) Complexes

No.	Complex	%Wt. loss Calcd. (Found)	Assignments	E^0	ΔH^0	ΔS^0 X 10^{-3}	ΔG^0	LogZ
1	[Co (AEMHPPS)$_2$(H_2O)$_2$]. H_2O	5.62 (5.51)	Loss of oneH_2O Lattice and two coord. H_2O	4293.1	-1.12	2.41	0.137	13.71
		44.12 (44.31)	Loss of one molecule of ligand	4640.3	1.81	-3.57	-0.235	13.83
		(17.80) 18.10	Loss of $C_4H_3N_2NH_2 + CH_4$	7012.2	-5.44	8.70	2.24	13.91
6	[Co(HMOEMPS). (H_2O)$_2$]	6.0 (5.95)	Loss of two coord. H_2O	4755.2	-0.06	1.13	1.64	13.55
		27.16 (27.47)	Loss of $C_4H_3N_2NHSO_2H + 2$ H_2	6031.1	-4.21	7.63	1.37	13.52
12	[Co (AMOPPS)].(½H_2O)	1.63 (1.61)	Loss of ½ H2O lattice	4365	0.28	6.112. 10^{-4}	0.025	13.69
		32.49 (32.61)	Loss of $C_4H_3N_2NHSO_2H$ + $CH_4 + 2$ H_2	4787.03	-0.37	7.584.10^{-4}	0.041	13.6 4

Table 4: Antibacterial and antifungal activity of the ligands (L_1 – L_4) and their complexes

Compound	Staphylococcus aureus (SA) G (+Ve)	Escherichia coli (EC) G (-Ve)	Candida albicans (CA) (fungus)	Aspergillusflavus (AF) (fungus)
L_1	13	15	14	16
Complex 1	11	12	13	14
Complex 3	18	20	21	19
L_2	15	16	13	12
Complex 4	12	11	11	13
Complex 5	19	20	18	20
L_3	14	15	13	12
Complex 8	11	12	10	10
Complex 9	18	17	21	20
L_4	16	17	15	14
Complex 10	10	9	8	11

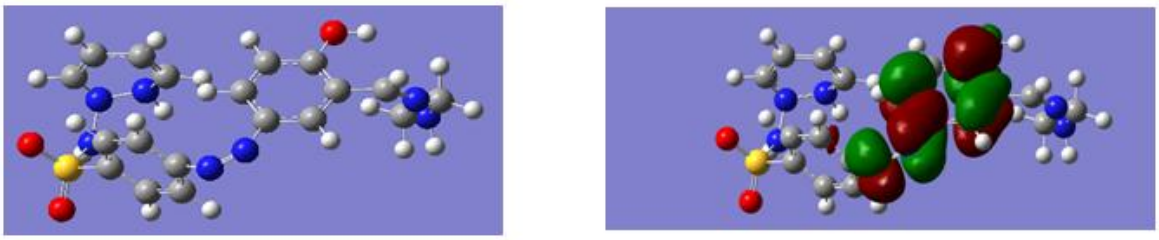

Fig.1: electron density function of azomethine group in L_1

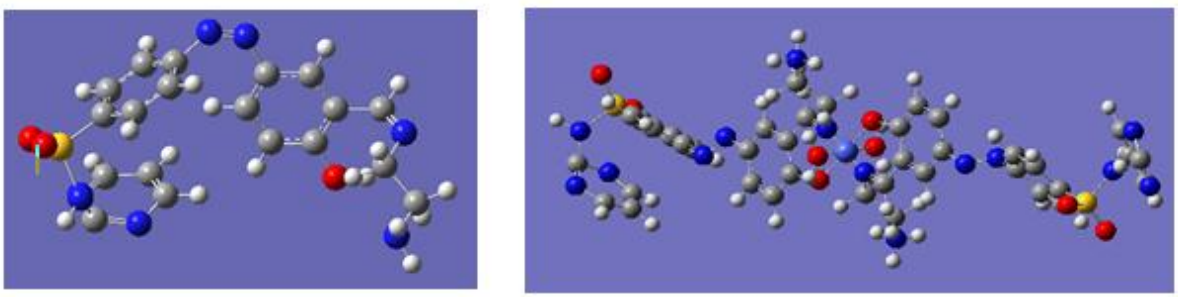

Ligand L_1 (a) **Complex 1 (b)**

Fig. 2: 3D modeling of the ligand L_1 and complex 1 using Gaussian program

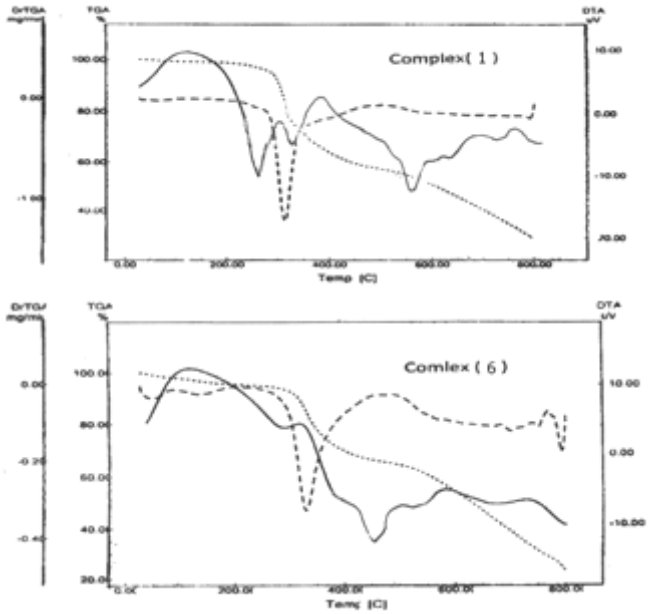

Fig. 3: Thermogravimetric curves of some Co(II) complexes

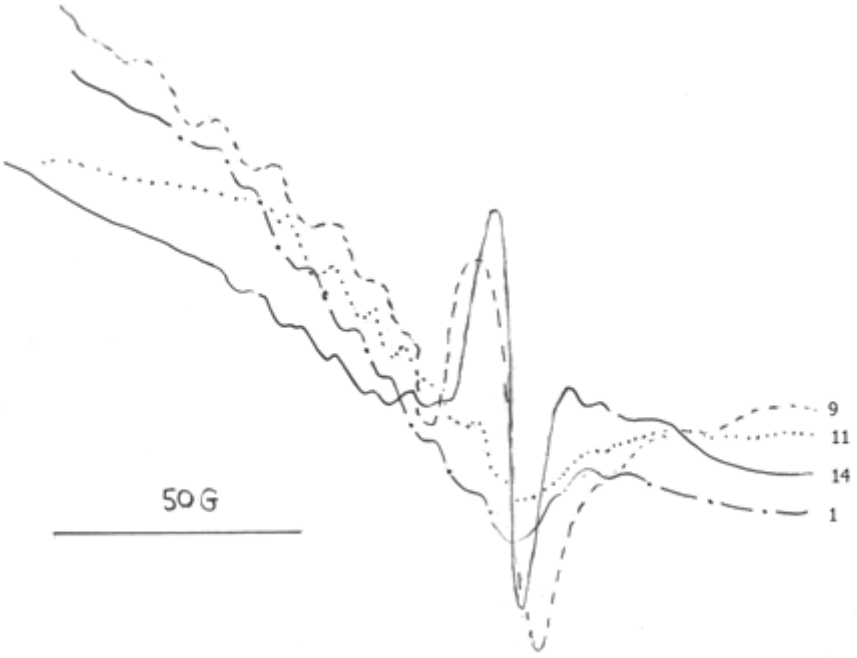

Fig. 4: ESR spectra of some Fe (III) and Co (II) complexes

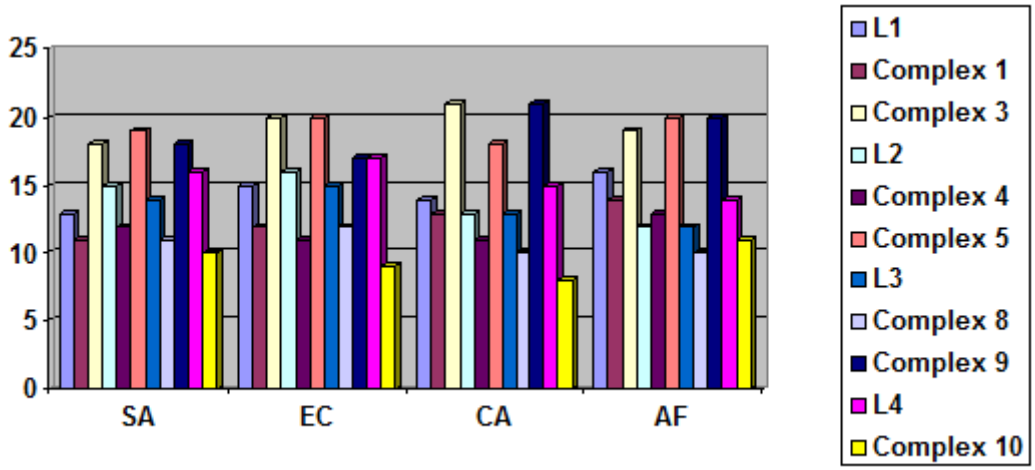

Fig. 5: Antibacterial and antifungal activity of the ligands (L_1–L_4) and some of their metal complexes

REFERENCES

1. EL-Ghamry H , Sakaiz K, Masaoka S , EL-Baradie K and Issa R . J Coord Chem. 2012;65:780.
2. Maurya RC and Rajput S. J Mol Struct. 2006;794:24–34.
3. Mubarak AT, El-Sonbati AZ, El-Bindary AA, Issa RM and Kera HM. Appl Organomet Chem. 2006;20:819.
4. Nagpal P and Singh RV. Appl Organomet Chem. 2004;18:221–226.
5. Wu CY, Chen LH, Hwang WS, Chen HS and Hung CH. J Organomet Chem. 2004;689:2192–2200.
6. Singh HL, Varshney S and Varshney AK. Appl Organomet Chem. 1999;13:637–641.
7. Przybylski P, Huczynski A, Pyta K, Brzezinski B and Bartl F. Curr Org Chem. 2009;13:124–148.
8. Da Silva CM, Da Silva DL, Modolo LV, Alves RB, De Resende MA, Martins CVB and De Fatima A. J Adv Res. 2011;2:1–8.
9. Jain M, Gaur S, Singh VP and Singh RV. Appl Organomet Chem. 2004;18:73–82.
10. Vogel AI. Quantitative Inorganic Analysis Including Elemental Instrumental Analysis.1962 second ed. Longmans, London.
11. Tawfik MA, El-ghamry M A, Abu-El-Wafa SM and Ahmed NM. Spectrochimica Acta Part A. 2012; 97:1172–1180.
12. Bansol A and Singh RV. Indian J Chem Sect A. 2002;40:989.
13. Hanna WG and Moowad MM. Transition Met. Chem. 2001;26:644.
14. Sari N, Arslan S, Logoglu E and Sakiyan I. J Sci. 2003;16:283.
15. Ismail TMA. J Coord. 2006;59:255-270.
16. Ismail TMA. J Coord. 2005;58:141-151.
17. Stuart B. Infrared and Spectroscopy: Fundamentals and Applications, Wiley 621Interscience. 2003 New York.
18. Nakamoto K. Infrared and Ramen Spectra of Inorganic and Coordination Compounds, fourth ed. Wiley Interscience. 1986 New York.
19. Geary WL. Coord Chem Rev. 1971;81.
20. Stahl-Brad R and Low W. Phys Rev. 1959;113:775.
21. Gao ES, San BH and Liv S. Syn React Inorg Met Org Chem. 1997;27:115.
22. Beraldo H, Boyd LP and West DX. Trans Met Chem. 1998;23:67.
23. Abu-El-Wafa SM, El-Ris MA and Ahmed FA. Inorg Chem Acta. 1987; 136:127-131.
24. Mashaly MM, Ismail T MEL, Maraghy SB and Habib HA. J Coord Chem. 2004; 57:1099-1123.
25. Bodke Y and Sangapure SS. J Indian Chem Soc. 2003; 80:187.
26. Ismail TMA and Saleh AA. Egypt J Chem. 2000;43:27.
27. Ismail TMA, Saleh AA and EL Ghamry MA. Spectrochimica Acta Part A. 2012 ;86: 276
28. Coats AW and Redfern JP. Nature. 1964; 20:68.
29. Abu El- Wafa S M , Gaber M, Issa RM and Ismail TM. Bull Soc Chem Fr. 1988; 1: 31.
30. Cotton FA, Gave DMI and Sacce A. J Am Chem Soc. 1961; 83:4175.
31. Polter WC and Taylor LT. Inorg Chem. 1976;15:88.

32. Wendlandt WW. Thermal Methods of Analysis. 2 nd edn. 1973 Wieky .
33. Saleh AA, Tawfik AM, Abu El- Wafa SM and Osman HF. J Coord Chem. 2004; 57:191.
34. Fidone I and Stevens KWH. Proc Phys. 1959 ;73.
35. Bodke Yand Sangapure SS. J Indian Chem Soc. 2003;80 :187.
36. Abu El- Wafa SM and Issa RM. Bull Soc Chim Fr. 1989;37: 88.
37. Neelakantan MA, Ray FR and Pillai MS. J Indian Chem Soc. 2008; 85:100.
38. Dayalan A, Meera P, Balaraju K, Agastian P and Ignasimuthu S. J Indian Chem Soc. 2009;86:628.
39. Shikkargol RK, Mallikarjuna NN and Angadi SD. Natl Acad Sci Lett. (India) 2001; 24:39–43.
40. Sengupta SK, Pandy OP, Srivastava BK and Sherma VK. Transition Met Chem. 1998;23:349.
41. Kumar S, Dhar DN and Saxena PN. J Sci Ind Res. 2009;68:181–187.
42. Mohamed GG, Omar MM and Hindy AM. Turk J Chem. 2006;30:361–382.
43. Sing K, Barwa MS and Tyagi P. Eur J Med Chem. 2006;41:147–153.
44. Shanson DC. Microbiology in Clinical Practice. Wright PSG. 1982 Bristol, London, Boston.